A COMPLETE CHARACTERIZATION AND SOLUTION TO THE MICROPHONE POSITION SELF-CALIBRATION PROBLEM

Yubin Kuang, Simon Burgess, Anna Torstensson and Kalle Åström

Centre for Mathematical Sciences, Lund University
{yubin,simonb,annat,kalle}@maths.lth.se

ABSTRACT

This paper presents a complete characterization and solution to microphone position self-calibration problem for time-of-arrival (TOA) measurements. This is the problem of determining the positions of receivers and transmitters given all receiver-transmitter distances. Such calibration problems arise in application such as calibration of radio antenna networks, audio or ultra-sound arrays and WiFi transmitter arrays. We show for what cases such calibration problems are well-defined and derive efficient and numerically stable algorithms for the minimal TOA based self-calibration problems. The proposed algorithms are non-iterative and require no assumptions on the sensor positions. Experiments on synthetic data show that the minimal solvers are numerically stable and perform well on noisy data. The solvers are also tested on two real datasets with good results.

***Index Terms*—** Time-of-Arrival, Network Calibration, Microphone Self-Calibration, Minimal Solver

1. INTRODUCTION

The problem of sensor network self-calibration is essential to localization and navigation. In this paper we focus on the time-of-arrival (TOA) based self-calibration problem, i.e. the problem of determining the positions of a number of receivers and transmitters given all receiver-transmitter distances. This problem has certain similarities to the problem of determining a set of points given all inter-point distances, which is usually solved using multi-dimensional scaling [1]. Such problems are of general interest in visualization and analysis of large datasets and for many geometric problems. It also relates to the study of sensor networks under rigid graph theory [**?**, 2] where general graph structure is of interest. The TOA-based self-calibration problem studied here corresponds to a special case - bipartite graph [3]. It is important for network calibration using e.g. microphone arrays, given recordings of sounds emitted at unknown locations, to microphones at unknown positions, determine both sound emission positions and microphone locations.

Such problems could be solved using alternative techniques, such as manually measuring all distances between microphones or using computer vision. Examples of such approaches are given in [4–9]. Here we argue that efficient solution to the TOA-based self-calibration problem opens up new technological possibilities e.g. calibration of a sensor network on the fly, determining of reflections of receivers and transmitters while moving in an unknown terrain etc. The solution of the problem is also of great theoretical interest and the solution techniques are interesting per se.

The research leading to these results has received funding from the strategic research projects ELLIIT and eSSENCE, and Swedish Foundation for Strategic Research projects ENGROSS and VINST(grant no. RIT08-0043).

Iterative methods exist for TOA or time-difference-of-arrival (TDOA) based self-calibration [10, 11]. However, such methods can get stuck in local minima which are dependent on initialization. Non-iterative methods for initializing network self-calibration have received less attention. For general graph structure, one can relax the TOA-based calibration problem as a semi-definite program [12]. For bipartite graph, initialization of TOA-based bipartite networks studied in [13], where solutions to the minimal case of 3 transmitters and 3 receivers in the plane is given. Initialization of time-difference-of-arrival (TDOA) networks is studied in [14] where a solution to non-minimal case of 10 receivers and 4 transmitters in 3D for TOA problem was also derived. In [15, 16] a solution is given to the TOA based self-calibration problem, if one may additionally assume that one of the receivers coincide with the position of one of the transmitters. In [17] and refined in [18] a far field approximation was utilized to initialize both TOA and TDOA problems. In [19, 20], algorithms for far-field unsynchronized receivers were also proposed. All these previous works attempt to solve the problem with either minimal or close to minimal data. Studying these minimal cases is both of theoretical importance and essential to develop fast stable algorithms suitable in RANSAC [21] and other solution schemes.

In this paper, we completely characterize the TOA based self-calibration problem in three dimensions. It is shown that such problems are well-defined for m receivers and n transmitters if and only if $m \geq 4$, $n \geq 4$, $m + n \geq 10$. We present efficient, numerically stable and non-iterative algorithms for such problems. In particular, we study the minimal problem of $(m = 6, n = 4)$ (or $(m = 4, n = 6)$ which is identical because of symmetry). We show that this problem has in general 38 solutions and present an algorithm for determining these 38 solutions given an arbitrary 4×6 matrix of distance measurements. Furthermore we study the the problem of $(m = 5, n = 5)$. We show that each 5×5 matrix must fulfill one constraint. But as long as this one constraint is fulfilled the problem is minimal and has 42 solutions. Also for this problem we provide a fast and numerically efficient algorithm. To the best our knowledge, our algorithms are the first to give practical numerical solution for minimal TOA calibration problems in 3D. We also extend the solution scheme to overdetermined cases and sketch how the technique could be extended to other dimensions.

2. THE TOA-BASED CALIBRATION PROBLEM

Let $\mathbf{r}_i$, $i = 1, \ldots, m$ and $\mathbf{s}_j$, $j = 1, \ldots, n$ be the spatial coordinates of m receivers (e.g. microphones) and n transmitters (e.g. sound events), respectively. For measured time of arrival t_{ij} from transmitter $\mathbf{r}_i$ and receiver $\mathbf{s}_j$, we have $vt_{ij} = ||\mathbf{r}_i - \mathbf{s}_j||_2$ where v is the speed of measured signals. We assume that v is known and constant, and that we at each receiver can distinguish which transmitter j each event is originating from. This can be done e.g. if the signals are temporally separated or by using different frequencies. We will in the sequel work with the distance measurements $d_{ij} = vt_{ij}$. The TOA calibration problem can then be defined as follows.

Problem 1 *(Time-of-Arrival Self-Calibration) Given absolute distance measurements d_{ij} determine receiver positions $\mathbf{r}_i$, $i = 1, \ldots, m$ and transmitter positions $\mathbf{s}_j$, $j = 1, \ldots, n$ such that $d_{ij} = ||\mathbf{r}_i - \mathbf{s}_j||_2$.*

Note that for such problems, one can only reconstruct locations of receivers and transmitters up to euclidean transformation and mirroring, henceforth referred to as the gauge freedom. In the following discussion, we assume that the dimensionality of the affine space spanned by $\mathbf{r}_i$ and $\mathbf{s}_j$ is the same and it is denoted as K, typical values in practice is $K = 3$ for transmitters and receivers in general 3D positions. The minimal cases for different dimensions have previously been determined in [3, 13]. Here we define a *minimal case* to a problem as the case that consists of the minimal set of constraints or equations such that the problem generally has finite number of solutions. It is relatively straightforward to calculate the number of degrees of freedom in the measurements, mn and the number of degrees of freedom in the manifold of unknown parameters, e.g. $3n+3m-6$ for TOA in 3D. To be more precise one has to study the equations using algebraic geometry, to make certain that there are no anomalies in the set of equations.

2.1. Analysis of the TOA-based Calibration Problem

In this section, we analyze the minimal cases for TOA-based self-calibration problem. We start by deriving a set of new equations.

Since the distance measurements are assumed to be real and positive one does not lose any information by squaring them, i.e.

$$d_{ij}^2 = (\mathbf{r}_i - \mathbf{s}_j)^T(\mathbf{r}_i - \mathbf{s}_j) = \mathbf{r}_i^T\mathbf{r}_i + \mathbf{s}_j^T\mathbf{s}_j - 2\mathbf{r}_i^T\mathbf{s}_j.$$

Notice that these are now polynomial equations in the unknowns. The problem is significantly easier to analyze and solve by forming new equations according to the following linear combinations of d_{ij}^2:

$$\begin{pmatrix} d_{11}^2 & d_{12}^2 - d_{11}^2 & \ldots & d_{1n}^2 - d_{11}^2 \\ d_{21}^2 - d_{11}^2 & & & \\ \ldots & & \tilde{\mathbf{D}} & \\ d_{m2}^2 - d_{11}^2 & & & \end{pmatrix}, \quad (1)$$

where $\tilde{\mathbf{D}}$ is a $(m-1)(n-1)$ matrix with entries as $\tilde{d}_{ij} = d_{i,j}^2 - d_{i1}^2 - d_{1j}^2 + d_{11}^2$, with $i = 2, \ldots m$ and $j = 2, \ldots, n$.

These new mn equations are equivalent to the mn equations formed by d_{ij}^2. The new ones are in fact an invertible linear combinations of the old ones.

These equations are of four types:

(A) 1 equation $d_{11}^2 = (\mathbf{r}_1 - \mathbf{s}_1)^T(\mathbf{r}_1 - \mathbf{s}_1)$.

(B) $n-1$ equations of type $d_{1j}^2 - d_{11}^2 = \mathbf{s}_j^T\mathbf{s}_j - \mathbf{s}_1^T\mathbf{s}_1 - 2\mathbf{r}_1^T(\mathbf{s}_j - \mathbf{s}_1)$, for $j = 2, \ldots n$.

(C) $m-1$ equations of type $d_{i1}^2 - d_{11}^2 = \mathbf{r}_i^T\mathbf{r}_i - \mathbf{r}_1^T\mathbf{r}_1 - 2(\mathbf{r}_i - \mathbf{r}_1)^T\mathbf{s}_1$, for $i = 2, \ldots m$.

(D) $(m-1)(n-1)$ equations of type $d_{ij}^2 - d_{i1}^2 - d_{1j}^2 + d_{11}^2 = -2(\mathbf{r}_i - \mathbf{r}_1)^T(\mathbf{s}_j - \mathbf{s}_1)$, for $i = 2, \ldots m, j = 2, \ldots n$.

Without loss of generality we may assume that $m \geq n$. It turns out that the characterization of the problem depends on the affine span of the transmitters and the receivers. For simplicity we will in the following concentrate on 3D problems and will assume that the affine span of both the transmitters and of the receivers are of dimension 3. Notice, however, that much of the argumentation and theory is straightforward to generalize to other dimensions. A brief sketch on what can be said in other dimensions is given in Section 2.4.

The solution strategy is to use the equations of type D first and use factorization techniques to solve for $\mathbf{r}$'s and $\mathbf{s}$'s up to a translation vector $\mathbf{b}$ (3 degrees of freedom) and an affine deformation $\mathbf{L}$ (6 degrees of freedom up to an unknown rotation). By a clever choice of parametrization of the problem it can be shown that the equations of Type C are linear in the unknowns and the equations of Types A and B can be used to form polynomial equations. We will then show that such problems are well defined and can be solved if $m \geq 4$, $n \geq 4$ and $m + n \geq 10$. The interesting minimal cases are thus $m = 6, n = 4$ (and $m = 4$, $n = 6$) as well as $m = 5$, $n = 5$. It was shown in [3] that these corresponding to rigid cases for bipartite graphs in 3D.

The factorization step can be understood as follows. Let $\mathbf{R}_i = \left[(\mathbf{r}_i - \mathbf{r}_1)\right]$ and $\mathbf{S}_j = \left[-2(\mathbf{s}_j - \mathbf{s}_1)\right]$. The equations of type D can be written as $\tilde{\mathbf{D}} = \mathbf{R}^T\mathbf{S}$ with $\mathbf{R}_i$ as columns of $\mathbf{R}$ and $\mathbf{S}_j$ as columns of $\mathbf{S}$. The ranks of $\mathbf{R}$ and $\mathbf{S}$ depends on the dimensionality of the affine span of the receivers and the transmitters respectively. As we assume that both of these are 3, then the matrix $\tilde{\mathbf{D}}$ also has rank 3. This also implies that in order to solve the problem, it is required that $m \geq 4$ and $n \geq 4$. By factorizing $\tilde{\mathbf{D}}$ which is of rank 3 using e.g. singular value decomposition, we can compute the vectors to all receivers and transmitters from unknown initial/reference positions ($\mathbf{r}_1$ and $\mathbf{s}_1$) up to an unknown full-rank 3×3 transformation $\mathbf{L}$ such that $\tilde{\mathbf{D}} = \tilde{\mathbf{R}}^T\mathbf{L}^{-1}\mathbf{L}\tilde{\mathbf{S}} = \mathbf{R}^T\mathbf{S}$.

To solve for the unknown transformation and reference positions, we now utilize the nonlinear constraints in equations of Type A, B and C. First we can fix the translational part of the gauge freedom by choosing the location $\mathbf{r}_1$ at the origin. Given that $\mathbf{R} = \mathbf{L}^{-T}\tilde{\mathbf{R}}$ and $\mathbf{S} = \mathbf{L}\tilde{\mathbf{S}}$, we can parameterize $\mathbf{s}_1$ as $\mathbf{L}\mathbf{b}$ where $\mathbf{b}$ is a 3×1 vector. This gives

$$\begin{aligned} &\mathbf{r}_1 = \mathbf{0},\ \mathbf{s}_1 = \mathbf{L}\mathbf{b} \\ &\mathbf{r}_i = \mathbf{L}^{-T}\tilde{\mathbf{R}}_i,\ i = 2\ldots m \\ &\mathbf{s}_j = \mathbf{L}(\tilde{\mathbf{S}}_j^* + \mathbf{b}),\ j = 2\ldots n, \end{aligned} \quad (2)$$

where $\tilde{\mathbf{S}}_j^* = \tilde{\mathbf{S}}_j/(-2)$. Using this parametrization the equations of type (A), (B) and (C) become

$$\begin{aligned} d_{11}^2 &= (\mathbf{r}_1 - \mathbf{s}_1)^T(\mathbf{r}_1 - \mathbf{s}_1) = \mathbf{s}_1^T\mathbf{s}_1 \\ &= \mathbf{b}^T\mathbf{L}^T\mathbf{L}\mathbf{b}, && (3) \\ d_{1j}^2 - d_{11}^2 &= \mathbf{s}_j^T\mathbf{s}_j - \mathbf{s}_1^T\mathbf{s}_1 \\ &= \tilde{\mathbf{S}}_j^{*T}\mathbf{L}^T\mathbf{L}\tilde{\mathbf{S}}_j^* + 2\mathbf{b}^T\mathbf{L}^T\mathbf{L}\tilde{\mathbf{S}}_j^*, && (4) \\ d_{i1}^2 - d_{11}^2 &= \mathbf{r}_i^T\mathbf{r}_i - 2\mathbf{r}_i^T\mathbf{s}_1 \\ &= \tilde{\mathbf{R}}_i^T(\mathbf{L}^T\mathbf{L})^{-1}\tilde{\mathbf{R}}_i - 2\mathbf{b}^T\tilde{\mathbf{R}}_i. && (5) \end{aligned}$$

Observe that all the constraints involve only $\mathbf{L}^T\mathbf{L}$ (and its inverse) and $\mathbf{b}$. By representing $(\mathbf{L}^T\mathbf{L})^{-1}$ with a symmetric matrix $\mathbf{H}$ parameterized with 6 unknowns, the constraints in (3), (4) and (5) can then be simplified as

$$\begin{aligned} d_{11}^2 &= \mathbf{b}^T\mathbf{H}^{-1}\mathbf{b}, && (6) \\ d_{1j}^2 - d_{11}^2 &= \tilde{\mathbf{S}}_j^{*T}\mathbf{H}^{-1}\tilde{\mathbf{S}}_j^* + 2\mathbf{b}^T\mathbf{H}^{-1}\tilde{\mathbf{S}}_j^*, && (7) \\ d_{i1}^2 - d_{11}^2 &= \tilde{\mathbf{R}}_i^T\mathbf{H}\tilde{\mathbf{R}}_i - 2\mathbf{b}^T\tilde{\mathbf{R}}_i. && (8) \end{aligned}$$

With this parameterization, there are in total 9 unknowns (6 and 3 unknowns for $\mathbf{H}$ and $\mathbf{b}$, respectively). By utilizing $\mathbf{H}^{-1} = \mathrm{adj}(\mathbf{H})/\det(\mathbf{H})$, where $\mathrm{adj}(\mathbf{H})$ is the adjoint of $\mathbf{H}$, we can multiply equations in (6) and (7) by $\det(\mathbf{H})$ to rewrite them as polynomials equations. In this case, we have $(n + m - 1)$ equations, among which the $(m-1)$ equations in (8) are linear, the $(n-1)$ equations in (7) are polynomial equations of degree 3 and Equation (6) is of degree 4. Thus we need $n+m-1 \geq 9$ or $n+m \geq 10$ in order to solve for the 9 unknowns. Since both $m \geq 4$ and $n \geq 4$ there are two minimal cases $6r/4s$ ($4r/6s$) and $5r/5s$.

2.2. Solving the Polynomial System

For the minimal case of 6 receivers and 4 transmitters, there are 5 linear equations of type C. By linear elimination we can express $\mathbf{H}$ and $\mathbf{b}$ in terms of $9-5=4$ unknowns $\mathbf{x}=(x_1,x_2,x_3,x_4)$. We now obtain four equations

$$\det(\mathbf{H})d_{11}^2 = \mathbf{b}^T \operatorname{adj}(\mathbf{H})\mathbf{b} \tag{9}$$

$$\det(\mathbf{H})(d_{12}^2 - d_{11}^2) = \tilde{\mathbf{S}}_2^{*T} \operatorname{adj}(\mathbf{H})\tilde{\mathbf{S}}_2^* + 2\mathbf{b}^T \operatorname{adj}(\mathbf{H})\tilde{\mathbf{S}}_2^* \tag{10}$$

$$\det(\mathbf{H})(d_{13}^2 - d_{11}^2) = \tilde{\mathbf{S}}_3^{*T} \operatorname{adj}(\mathbf{H})\tilde{\mathbf{S}}_3^* + 2\mathbf{b}^T \operatorname{adj}(\mathbf{H})\tilde{\mathbf{S}}_3^* \tag{11}$$

$$\det(\mathbf{H})(d_{14}^2 - d_{11}^2) = \tilde{\mathbf{S}}_4^{*T} \operatorname{adj}(\mathbf{H})\tilde{\mathbf{S}}_4^* + 2\mathbf{b}^T \operatorname{adj}(\mathbf{H})\tilde{\mathbf{S}}_4^* \tag{12}$$

in the four unknowns. Here both $\mathbf{H}$ and $\mathbf{b}$ depend on $\mathbf{x}$. Using tools from algebraic geometry it can be shown that the solution set to equations (9-12) in general consists of a set of dimension 1 (a curve) of 'false' solutions that fulfill $\det(H)=0$ and 38 points. This is done by running the system of equations in Macaulay2 [22] over the field of $\mathbb{Z}^p$, where p is a large prime number and with coefficients initialized randomly. To remove the one-dimensional curve of false solutions we employ a saturation technique as follows. We rewrite the equations using an additional unknown z and an additional equation $\det(\mathbf{H})=z$, i.e.

$$z d_{11}^2 = \mathbf{b}^T \operatorname{adj}(\mathbf{H})\mathbf{b} \tag{13}$$

$$z(d_{12}^2 - d_{11}^2) = \tilde{\mathbf{S}}_2^{*T} \operatorname{adj}(\mathbf{H})\tilde{\mathbf{S}}_2^* + 2\mathbf{b}^T \operatorname{adj}(\mathbf{H})\tilde{\mathbf{S}}_2^* \tag{14}$$

$$z(d_{13}^2 - d_{11}^2) = \tilde{\mathbf{S}}_3^{*T} \operatorname{adj}(\mathbf{H})\tilde{\mathbf{S}}_3^* + 2\mathbf{b}^T \operatorname{adj}(\mathbf{H})\tilde{\mathbf{S}}_3^* \tag{15}$$

$$z(d_{14}^2 - d_{11}^2) = \tilde{\mathbf{S}}_4^{*T} \operatorname{adj}(\mathbf{H})\tilde{\mathbf{S}}_4^* + 2\mathbf{b}^T \operatorname{adj}(\mathbf{H})\tilde{\mathbf{S}}_4^* \tag{16}$$

$$\det(\mathbf{H}) = z \tag{17}$$

We then multiply all equations with monomials in $\mathbf{x}$ up to degree 9 and keep the highest degree of z as 1. By doing this one can construct 966 equations involving 715 monomials which do not contain z and 210 monomials that do contain z. These equations can be represented by a sparse coefficient matrix $\mathbf{M} = [\mathbf{M}_0 \;\; \mathbf{M}_z]$ of size 966×925, where the coefficients corresponding to monomials without z are in $\mathbf{M}_0$ and those corresponding to monomials with z are in $\mathbf{M}_z$. After multiplication with $\mathbf{Q}^T$, where $\mathbf{QR} = \mathbf{M}_0$ is the QR-factorization of $\mathbf{M}_0$, we obtain

$$\mathbf{Q}^T\mathbf{M} = [\mathbf{R} \;\; \mathbf{Q}^T\mathbf{M}_z].$$

Here the last 336 rows of $\mathbf{R}$ is zero and thus the last 336 equations can all be written $z f_k(\mathbf{x}) = 0$. After division with z, we obtain 336 equations of degree 6 in $\mathbf{x}$. It can be shown that this solution set to these equations consist of 38 points.

We then use these equations for solving for the 38 solutions using a technique described in [23]. This involves generating corresponding coefficient matrix, row manipulation in order to generate a 38×38 matrix, whose eigenvalues and eigenvectors contain the solution to the system of polynomial equations. For each such solution, we then calculate $\mathbf{H}$ and $\mathbf{b}$ and then generate the solutions for $\mathbf{r}_i$ and $\mathbf{s}_j$ according to (2), finding $\mathbf{L}^{-1}$ by e.g. cholesky factorization of $\mathbf{H}$. $\mathbf{L}$ is thus only determined up to a matrix R where $R^T R = I$, which coincides with the gauge freedom of rotating and/or mirroring our solution. The 4r/6s case can be solved in the same way by first transposing the measurement matrix.

The case of 5 receivers and 5 transmitters is interesting. It is an overdetermined case in the sense that there are 25 measurements and 24 degrees of freedom in the solutions set. There is thus one constraint that has to be satisfied, i.e. the constraint that the 4×4 matrix $\tilde{\mathbf{D}}$ has determinant zero. However for all such data, the problem of determining $\mathbf{H}$ and $\mathbf{b}$ is minimal. There are $m+n-1=9$ equations (1 of Type A, 4 of Type B and 4 of Type C) and 9 unknowns. We follow a similar solution scheme as for the (6r/4s) case. By linear elimination using the 4 linear constraints of type C, we can express $\mathbf{H}$ and $\mathbf{b}$ in terms of $9-4=5$ unknowns $\mathbf{x} = (x_1,x_2,x_3,x_4,x_5)$. The remaining five constraints (1 of Type A, and 4 of Type B) give a polynomial system with 42 solutions after a saturation procedure similar to the previous case. Again we use the scheme in [23] to produce a numerically stable and efficient solution.

2.3. Overdetermined cases

For overdetermined cases ($m \geq 4, n \geq 4, m+n > 10$), the solver can be based on solving a minimal case, extending with trilateration, followed by non-linear optimization to obtain the maximum likelihood estimate. An alternative is to find the best rank 3 approximation of $\tilde{\mathbf{D}}$, solution of $\mathbf{H}$ and $\mathbf{b}$ using algebraic methods, and then again followed by non-linear optimization. An advantage with the former approach is that it can more easily be modified using RANSAC to remove potential outliers in the measurement matrix $\mathbf{D}$.

2.4. Higher and lower dimensional cases

The ideas presented here can relatively easy to generalized to other dimensions. The one-dimensional case is trivial. Only one measurement is needed to solve for the problem. In two dimensions the same approach can be used to show that one needs $m \geq 3, n \geq 3, m+n \geq 6$, which indicate only one minimal problem $3s/3r$. This was in fact solved with a different approach by Stewenius and Nister in [13] . The problem has in general 4 solutions. For dimension 4, the analysis gives $m \geq 5, n \geq 5, m+n \geq 15$, which gives minimal cases $5s/10r, 6s/9r, 7s/8r$,

3. EXPERIMENTS

We test our proposed algorithms on both synthetic and real data. The recovered sensor positions are up to unknown rotation and translation. We first determine the rotation and translation with least square fitting over the ground truth positions and then compute the errors. For synthetic data, we simulate the positions of receivers and transmitters as 3D points with independent Gaussian distribution of zero mean and identity covariance matrix. The 6r/4s solver always produce 38 solutions although some of these could be complex. Similarily the 5r/5s always produce 42 solutions. There are two steps in the algorithm where the solution could become non-real. First a solution to the system of polynomial equation could be non-real and secondly even if this solution is real the matrix $\mathbf{H}$ although real, could be indefinite in which case the Cholesky factorization becomes non-real. In Fig.1 (Left) is shown a histogram over 5000 simulations. As can be seen in the figure, for both solvers, there are usually between 14 and 24 real solutions to the system of polynomial equations, whereas only a few (most often less than 6) of these produce positive definite matrices $\mathbf{H}$), so that there is typically less than 6 real and thus valid solutions. This number is however data dependent. For noise-free synthetic data, we can see in Fig.1 (Right) that both the 6r/4s solver

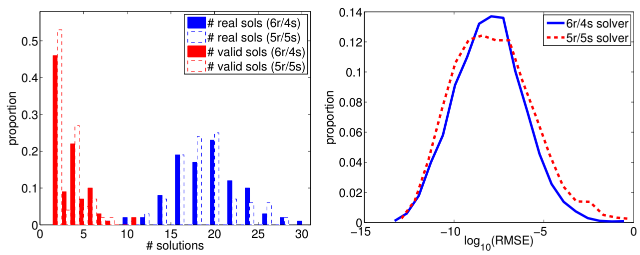

Fig. 1. Minimal solver performance on 5000 noise-free random synthetic TOA problems. Left: Distribution of the number of real and valid solutions each run produces, showing the relative frequency of number of real and valid solutions among the 38 (or 42) solutions. Right: the error distribution (RMSE) of reconstructed positions of microphone and sound sources.

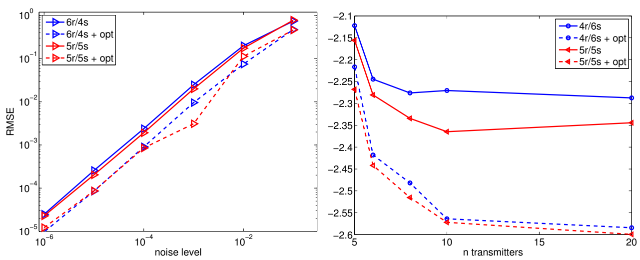

Fig. 2. Performance on noisy synthetic data - average errors (RMSE) of reconstructed positions of receivers and transmitters Left: minimal solvers (4r/6s and 5r/5s) under varying noise levels. Right: 10 receivers and varying number of transmitters under Gaussian noise with standard deviation 2×10^{-3}.

and 5r/5s solver are numerically stable. We also tested both solvers on data under different noise level and we observe that the solvers gives fairly good solutions under reasonable level of noise (Fig.2, left, solid lines). Using the solutions from the minimal solvers as initial solutions, we also apply nonlinear optimization step where we minimize $\sum_{ij}\left(d_{ij} - (||\mathbf{r}_i - \mathbf{s}_j||_2)\right)^2$ (Fig.2, dash lines). We also test the solvers on over-determined cases with fixed noise level, $m = 10$ and varying n (Fig.2, right). We can see that as n increases, both solvers gives better initial solutions for the reconstruction. The current implementation run at around $200ms$ and $800ms$ for $6r/4s$ and $5r/5s$ respectively, on a Macbook Air (1.8 GHz Intel Core i5 and 8 GB memory)[1].

For real experiments, we have used a publicly available dataset [15] for comparison as well as our own TOA measurements. In the dataset [15], the distances between the 8 microphones and 21 sounds are estimated based on the time-of-arrival measurements. The first microphone is assumed to be at the same location as first sound. For our algorithm, no such assumption is needed. To verify this, we simply remove the distance measurements corresponding to the first microphone and first sound, which gives us a 7×20 matrix. For this reduced set of measurements, the root mean square errors (RMSE) of our reconstructed positions of microphones and sound sources after non-linear iterative optimization are $0.0083m$ and $0.0108m$, respectively. This is similar to the accuracy [15] that achieves ($0.0091m$ for microphones and $0.0111m$ for sound sources) with the additional assumption. For the full set of data (8 microphones and 21 sounds), our solvers also gives similar errors as in [15]. Another set of real data was obtained using seven T-bone MM-1 microphones and five Roxcore portable speakers, connected to a Fast Track Ultra 8R sound card in an indoor environment, with speakers and microphones placed in an approximate $1.5 \times 1.5 \times 1.5\ m^3$ volume (Fig.3, Left). TOA measurements were obtained by heuristically matching sounds from different speakers to sound flanks recorded from different microphones. For this set of measurement, we also reconstructed the scene using computer vision based algorithms as ground truth. The reconstruction (Fig.3, Right) when compared to the vision-based reconstruction has RMSE $0.0088m$ and $0.0131m$ for microphones and speakers respectively.

[1]The solvers are available for download at http://www2.maths.lth.se/vision/downloads/.

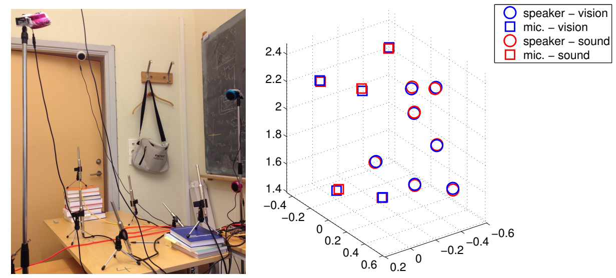

Fig. 3. Real microphone and speaker calibration setup, Left: the setup of microphones and speakers in an office, Right: the reconstructed sensor positions using TOA measurements (red) aligned with the positions estimated based on computer vision (blue).

4. RELATION TO PRIOR WORK

The most related works to ours are [15, 16], where the same factorization step is described. However, instead of solving the original problem, they solve a problem with an additional assumption that one receiver and one transmitter have identical positions. This work does not need this constraint, and is applicable to a wider set of problems. Close to our setting are also [13], where the minimal TOA calibration problem in 2D is solved, using three receivers and transmitters each, [14] which solves as a by-product the TOA calibration problem in 3D with a non-minimal configuration of 10 receivers and 4 transmitters and [18] which solves the TOA calibration problem assuming a far field approximation with a minimal configuration of 3 receivers and 6 transmitters. Thus no previous work has solved the minimal cases for general TOA-based self-calibration in 3D.

5. CONCLUSIONS

In this paper, we completely characterize the TOA base self-calibration problem in three dimensions. It is shown that such problems are well-defined for m receivers and n transmitters if and only if $m \geq 4$, $m \geq 4$, $m + n \geq 10$. We present practical and non-iterative solution algorithms for such problems. In particular, we present algorithms for solving the $(m = 6, n = 4)$ case (38 solutions) and the $(m = 5, n = 5)$ (42 solutions). For overdetermined cases we present two alternative approaches. The solution technique is general and can in principle be applied to higher dimensional problems. In the paper we show the applicability of the techniques to both simulated and real data. In the future it would be interesting to study how such algorithms could be used to further analyze problems within radio, Wi-Fi and ultrasound.

6. REFERENCES

[1] G. Young and A.S. Householder, "Discussion of a set of points in terms of their mutual distances," *Psychometrika*, vol. 3, no. 1, pp. 19–22, 1941.

[2] T. Eren, OK Goldenberg, W. Whiteley, Y.R. Yang, A.S. Morse, BDO Anderson, and PN Belhumeur, "Rigidity, computation, and randomization in network localization," in *INFOCOM 2004. Twenty-third AnnualJoint Conference of the IEEE Computer and Communications Societies*. IEEE, 2004, vol. 4, pp. 2673–2684.

[3] E.D. Bolker and B. Roth, "When is a bipartite graph a rigid framework," *Pacific J. Math*, vol. 90, no. 1, pp. 27–44, 1980.

[4] S. T. Birchfield and A.. Subramanya, "Microphone array position calibration by basis-point classical multidimensional scaling," *IEEE transactions on Speech and Audio Processing*, vol. 13, no. 5, 2005.

[5] D. Niculescu and B. Nath, "Ad hoc positioning system (aps)," in *GLOBECOM-01*, 2001.

[6] E. Elnahrawy, Xl. Li, and R. Martin, "The limits of localization using signal strength," in *SECON-04*, 2004.

[7] V. C. Raykar, I. V. Kozintsev, and R. Lienhart, "Position calibration of microphones and loudspeakers in distributed computing platforms," *IEEE transactions on Speech and Audio Processing*, vol. 13, no. 1, 2005.

[8] J. Sallai, G. Balogh, M. Maroti, and A. Ledeczi, "Acoustic ranging in resource-constrained sensor networks," in *eCOTS-04*, 2004.

[9] J. C. Chen, R. E. Hudson, and K. Yao, "Maximum likelihood source localization and unknown sensor location estimation for wideband signals in the near-field," *IEEE transactions on Signal Processing*, vol. 50, 2002.

[10] N.B. Priyantha, H. Balakrishnan, E. Demaine, and S. Teller, "Anchor-free distributed localization in sensor networks," in *Proceedings of the 1st international conference on Embedded networked sensor systems*. ACM, 2003, pp. 340–341.

[11] R. Biswas and S. Thrun, "A passive approach to sensor network localization," in *IROS 2004*, 2004.

[12] P. Biswas, T.C. Lian, T.C. Wang, and Y. Ye, "Semidefinite programming based algorithms for sensor network localization," *ACM Transactions on Sensor Networks (TOSN)*, vol. 2, no. 2, pp. 188–220, 2006.

[13] H. Stewénius, *Gröbner Basis Methods for Minimal Problems in Computer Vision*, Ph.D. thesis, Lund University, APR 2005.

[14] M. Pollefeys and D. Nister, "Direct computation of sound and microphone locations from time-difference-of-arrival data," in *Proc. of International Conference on Acoustics, Speech and Signal Processing*, 2008.

[15] M. Crocco, A. Del Bue, M. Bustreo, and V. Murino, "A closed form solution to the microphone position self-calibration problem," in *37th International Conference on Acoustics, Speech, and Signal Processing (ICASSP 2012), Kyoto, Japan*, March 2012.

[16] Marco Crocco, Alessio Del Bue, and Vittorio Murino, "A bilinear approach to the position self-calibration of multiple sensors," *Trans. Sig. Proc.*, vol. 60, no. 2, pp. 660–673, feb 2012.

[17] S. Thrun, "Affine structure from sound," in *Proceedings of Conference on Neural Information Processing Systems (NIPS)*, Cambridge, MA, 2005, MIT Press.

[18] Y. Kuang, E. Ask, S. Burgess, and K. Åström, "Understanding toa and tdoa network calibration using far field approximation as initial estimate," in *ICPRAM*, 2012.

[19] J. Wendeberg, F. Hoflinger, C. Schindelhauer, and L. Reindl, "Anchor-free tdoa self-localization," in *Indoor Positioning and Indoor Navigation (IPIN), 2011 International Conference on*, sept. 2011, pp. 1 –10.

[20] Simon Burgess, Yubin Kuang, and Kalle Åström, "Node localization in unsynchronized time of arrival sensor networks," in *Proceedings of the 21st International Conference on Pattern Recognition*, 2012.

[21] M. A. Fischler and R. C. Bolles, "Random sample consensus: a paradigm for model fitting with applications to image analysis and automated cartography," *Communications of the ACM*, vol. 24, no. 6, pp. 381–95, 1981.

[22] D. Grayson and M. Stillman, "Macaulay 2," Available at http://www.math.uiuc.edu/Macaulay2/, 1993-2002, An open source computer algebra software.

[23] Martin Byröd, Klas Josephson, and Kalle Åström, "Fast and stable polynomial equation solving and its application to computer vision," *Int. Journal of Computer Vision*, vol. 84, no. 3, pp. 237–255, 2009.